Journal of Geodesy (2004)
DOI 10.1007/s00190-004-0382-5

Journal of Geodesy

Calibration of GOCE SGG data using high–low SST, terrestrial gravity data and global gravity field models

J. Bouman[1], R. Koop[1], C. C. Tscherning[2], P. Visser[3]

[1] SRON National Institute for Space Research, Sorbonnelaan 2, 3584 CA Utrecht, The Netherlands
e-mail: j.bouman@sron.nl; Tel.: +31-30-253-5971; Fax: +31-30-254-0860
[2] Department of Geophysics, Juliane Maries Vej 30, 2100 Copenhagen, Denmark
[3] Delft Institute for Earth-Oriented Space Research, Kluyverweg 1, 2629 HS Delft, The Netherlands

Received: 3 June 2002 / Accepted: 27 January 2004 / Published online: 21 June 2004

Abstract. It is the aim of the GOCE mission to determine a model of the Earth's gravity field with high accuracy and resolution. For this purpose, gravity gradients will be measured in combination with high–low satellite-to-satellite tracking. The gravity gradients are derived from pair-wise differenced accelerations as determined by the six three-axes accelerometers that form the GOCE gradiometer. Since the measured accelerations suffer from errors of a random and systematic nature, the gravity gradients may suffer from random and systematic errors as well. Systematic errors are, for example, a scale factor and a bias. The common accelerations of the paired accelerometers also are contaminated with such errors. The common accelerations are used in the drag-free control of the satellite and are important for the separation of the gravitational and non-gravitational forces in the gravity field determination. The checking of the gravity gradients and the common accelerations against independent data (i.e. external to the GOCE satellite) in order to free the observations as well as is possible from systematic errors is called external calibration. The possibilities and limitations of using terrestrial gravity data and global gravity models for external calibration of the gravity gradients are reviewed. It turns out that the determination of a gravity gradient scale factor and bias using just the accurate knowledge of the central term and the flattening (J_2) of the Earth's gravity field is not good enough. When global gravity field models are used for the calibration, higher degrees and orders should be taken into account as well. With today's existing global models it seems to be possible to remove the greater part of the systematic errors of the GOCE gradients. A gravity gradient bias can accurately be recovered using terrestrial gravity data in a regional approach with least squares collocation. However, since regional data are used it may not be possible to determine calibration parameters valid for the whole (global) gravity gradient data set. Nevertheless, regional terrestrial gravity data could be used to validate the measured and calibrated gravity gradients. In addition, a possible use of GOCE high–low satellite-to-satellite tracking data to calibrate the common accelerations is explored; it is shown that this approach fails. If more accurate gravity field information becomes available then such a calibration may become feasible.

Key words: Gravity Field and Steady-State Ocean Circulation Explorer (GOCE) – Calibration – Gradiometry – Satellite-to-satellite tracking

Correspondence to: J. Bouman

1 Introduction

The main goal of the GOCE mission gravity field and steady-state ocean circulation explorer (expected to be launched 2006) is to provide unique models of the Earth's gravity field and of its equipotential surface, as represented by the geoid, on a global scale with high spatial resolution and to very high accuracy [European Space Agency (ESA) 1999]. For this purpose, GOCE will be equipped with a global positioning system (GPS) receiver for high–low satellite-to-satellite tracking (SST-hl) observations, and with a gradiometer for observation of the gravity gradients (SGG). The gradiometer consists of six three-axis accelerometers mounted in pairs along three orthogonal arms. From the readings of each pair of accelerometers the so-called common mode (CM) and differential mode (DM) signals are derived. The CM observations are used to obtain information about the linear accelerations and are input to the DFC (drag free control) system. The measurements of the CM are also needed for accurate separation of the gravitational and remaining non-gravitational forces in the

orbit determination process and are also important for the long wavelength gravity field recovery from SST measurements. The DM observations are used to derive the gravity gradients. The gradiometer is designed such as to give the highest achievable precision in the measurement bandwidth (MBW) between 5 and 100 mHz. For the diagonal gravity gradients ($\mathbf{V}_{XX}, \mathbf{V}_{YY}, \mathbf{V}_{ZZ}$) in a local orbital reference frame (LORF) (X-axis in the velocity direction, the Z-axis approximately radially outward and the Y-axis complementing the right-handed frame) the errors will not exceed 4 mE/$\sqrt{\text{Hz}}$ (1 E = 10^{-9} s^{-2}) in the MBW (Cesare 2002).

The measurements will be contaminated with stochastic and systematic errors (see e.g. SID, 2000; Cesare 2002). For the GOCE gradiometer, systematic errors typically are due to instrument imperfections such as misalignments of the accelerometers, scale factor mismatches, etc. Values for the absolute scale factors of the accelerometers (which are required to convert the accelerometer read-out voltages to m/s^2) are determined with an accuracy of 1% prior to the mission by the so-called on-ground calibration using a test bench. In addition, the CM and DM couplings, which are the result of such instrument imperfections, can be determined on the ground to a relative accuracy level of 10^{-2}–10^{-4}. Note that calibration is more than a removal of systematic errors due to instrument imperfections. It comprises also the conversion of the instrument read-outs (digital numbers) to physically sensible quantities in accordance with basic constants, standards and definitions. This is, however, not the topic of this paper, in which we will concentrate on the error in the observations instead.

A so-called internal calibration procedure has been proposed (ESA 1999), by which the CM and DM couplings can be determined to an accuracy level at which their effect on the gradients in the MBW stays below the required 4 mE/$\sqrt{\text{Hz}}$. The values of the calibration parameters (which are often referred to as the elements of the calibration matrix in which they are grouped) are measured by putting a known acceleration signal on the gradiometer in orbit using the thrusters (shaking). By 'calibration parameters' we mean here the scale factors, misalignment angles and couplings. After this procedure, the CM and DM read-outs of the gradiometer are corrected using the measured calibration parameters. The extreme accuracy level of the GOCE measurements may require the internal calibration procedure to be repeated each month, since there will be drifts due to, for example, temperature changes. Note that in order for the internal calibration procedure to work well, it must be ensured that the thrusters work according to the specifications and are calibrated themselves to a sufficient accuracy.

The gravity gradients are derived from the internally calibrated DM accelerations. The internal calibration, however, is not sensitive to all instrument imperfections, such as the read-out bias and the accelerometer mispositioning. Therefore, in order to possibly correct for remaining errors after internal calibration (outside or inside the MBW), a third calibration step is proposed which is called external calibration (or 'absolute' calibration). It is performed during or after the mission and typically makes use of external gravity data. In principle, not only gravity gradients may be externally calibrated, but also observations such as the CM accelerations, in order, for example, to improve the knowledge of the CM scale factors.

We will discuss our external calibration model in Sect. 2. In Sects. 3–5 three methods for external calibration are discussed. First of all, Sect. 3 considers the use of existing global gravity field information. Although GOCE is designed to deliver global gravity field information with unprecedented accuracy, the improvement is most noticeable in the MBW. Below the MBW, the GOCE gravity gradients may not be as accurate as existing or near future global gravity field information. Second, it is expected that in certain regions there is dense enough terrestrial gravity data with high enough accuracy to calibrate the GOCE gravity gradients in a regional approach. In Sect. 4 it is discussed how well a gravity gradient bias can be estimated using least squares collocation (LSC). Finally, the comparison of high–low SST data with the CM observations is reviewed. The CM observations are used in combination with the SST data to recover the long-wavelength gravity field. Conversely, it may be possible to check the CM observations from a combination of existing gravity field information and the SST data. Earlier results can be found in Arabelos and Tscherning (1998) and Koop et al. (2002).

Along with the external calibration of the observations themselves, their error needs to be assessed. Although important, error assessment is not discussed here [see e.g., Koop et al. (2002)]. Accurate calibration of gravity gradients, CM observations, etc. would in the ideal case lead to properly calibrated geoid heights and gravity anomalies, for example. These products can be compared with existing data sets of, for example, in-situ gravimetry observations in order to assess their accuracy. This process is referred to as validation. For a large part the same methods can be used as for external calibration, the difference being that validation provides information about the success of the calibration of the original measurements, but does not provide corrections to the data. Of course, different independent data sets should be used for validation and external calibration. Validation will not be discussed in detail here.

2 External calibration of gravity gradients

In this section we will start with the relation between the measured accelerations and the GOCE gravity gradients. The detailed relation between the measured accelerations, the CM and DM accelerations and the gravity gradients is given in the Appendix. Furthermore, the gradiometer instrument errors and the on-ground and internal calibration are briefly discussed in the Appendix. In this section we introduce the external calibration model for the gravity gradients, which is based on the error characteristics of the GOCE gravity gradients.

The gravity gradiometer consists of six three-axis accelerometers. The differenced accelerations (DM accelerations) between two accelerometers along one of the three axes of the LORF (arms of the gradiometer) contain contributions from accelerations due to the satellite angular velocity $\boldsymbol{\omega}$ and angular acceleration $\dot{\boldsymbol{\omega}}$, and due to the gravity gradients (for details, see the Appendix). From the DM accelerations, the gradiometer rotation and subsequently the gravity gradients in the LORF can be derived. Ideally, the three axes of one accelerometer are orthogonal and, for example, the x-axes of two accelerometers along the X-axis are parallel. Since in practice such an ideal situation does not occur, calibration is needed to determine instrument imperfections.

If it is assumed that the on-ground and internal calibration have been performed according to the specifications, then we may also assume that in the MBW the error of the gravity gradients is below the required level. However, this does not imply that no systematic errors are left in the gradients, either inside or outside the MBW. We can try to reduce the gradient error even further in order to improve the quality of the observations. For example, DM acceleration biases are not estimated at all in the on-ground or internal calibration and such biases lead to gravity gradient biases. Correct gravity gradients can therefore only be obtained using independent gravity field information in a next calibration step. This is the role of external calibration. Furthermore, the mispositioning of the accelerometers as well as the non-orthogonality of the physical gradiometer arms with respect to the LORF do not show up in the on-ground and internal calibration. These errors do however propagate to the estimated gravity gradients, and could perhaps be taken care of in the external calibration. Gravity gradients may also be contaminated with errors coming from the star-tracker observations, since these are required to determine the satellite angular velocity $\boldsymbol{\omega}$. The gravity gradients are derived from the DM accelerations and the angular velocity (see the Appendix). Finally, external calibration offers the possibility to remove large systematic errors below the MBW that are caused by the misalignment between the accelerometers and the LORF, etc. The on-ground and internal calibration are specified such that the errors in the MBW are below specified levels; below the MBW the specifications are much less stringent. Nevertheless, it is desirable to produce a gravity gradient that is as clean as possible. With independent gravity field information this can be taken care of. External calibration will be called 'calibration' in this paper from Sect. 3 onward.

We could question whether external calibration of the gravity gradients is necessary or even possible. In the MBW it is unlikely that there is more accurate external gravity field information available, while the larger error below the MBW is compensated by the SST data, which provide accurate long-wavelength information. However, the gravity gradients themselves are important and it is desirable to remove systematic errors as much as possible. Also, when the gradiometer data are combined with the SST data to compute geoid heights or gravity anomalies, it may be an advantage to have 'clean' gravity gradients in order to benefit as much as possible from the correct information content of the gradients. For example, the implementation of so-called ARMA filters, which account for the gradient error correlation, may profit from the reduction of systematic gradient errors (Schuh 2002).

The difference between the external calibration of gravity gradients and that of accelerations is that in the former case we try to reduce the net effect of instrument and other errors on the gravity gradients, while in the latter case we try to estimate accelerometer scale factors etc., which are more directly linked to the instrument. However, this would require a somewhat different calibration model as compared to internal calibration since, as explained above, not all instrument errors are included in the latter. More seriously, a proper external calibration requires the use of independent data. Such data are available for the gravity gradients but not for the accelerations. Besides the gravitational part of the accelerations, we also need independent information on the satellite rotation, which is not available. An additional complicating factor is that the DM accelerations, and hence their errors, are differenced, integrated, squared, and so on. It is therefore not straightforward how the DM errors propagate to gravity gradient errors, while the gravity gradients are the functionals we want to obtain. Hence we choose to calibrate gravity gradients.

The calibration model we use should be related to the gravity gradient errors. The accelerometer scale factor errors and biases result in similar gravity gradient errors, whereas the accelerometer non-orthogonality and misalignment project part of the signal (due to satellite rotation and the gradients themselves) onto the measured accelerations. Because the signal has most of its power at 1 and 2 cycles per revolution (cpr), the DM acceleration errors and the gravity gradient errors will also show 1, 2 etc. cpr errors. The mispositioning of the accelerometer pairs along the axes of the LORF directly results in gravity gradient scale factor errors, when the gradients are derived from the DM accelerations. In addition, the non-orthogonality of the gradiometer arms in the LORF (which is due to accelerometer mispositioning perpendicular to the LORF axes) again erroneously projects part of the signal onto the gravity gradients. Therefore, in a somewhat simplified but rather general approach, the time series of gravity gradients $\underline{\mathbf{y}}$ after internal calibration can be written as

$$\underline{\mathbf{y}}(t) = \lambda[\mathbf{y}_s(t) + \boldsymbol{\Delta}\mathbf{y} + \mathbf{y}' \cdot t + \sum_{k=1}^{K}(a_k \cos k\boldsymbol{\omega}(t) + b_k \sin k\boldsymbol{\omega}(t)) + \underline{\mathbf{n}}(t) + \text{other}] \quad (1)$$

where λ is the scale factor, $\mathbf{y}_s$ are the 'true' gravity gradients, $\boldsymbol{\Delta}\mathbf{y}$ is a constant offset (bias), $\mathbf{y}'$ is a trend, $\boldsymbol{\omega} = 2\pi t/T$, t is the time, T is the mean orbital period, a_k, b_k are Fourier coefficients, and $\underline{\mathbf{n}}$ is the observation noise. The term 'other' contains the remaining errors, such as outliers (neglected here). The number of unknowns is $3 + 2K$, i.e. a scale factor, bias, trend and

$2K$ Fourier coefficients. The trend is included to model, for example, slow bias variations in time, cf. CHAMP results (Reigber et al. 2003).

It should be noted that the external calibration of the gravity gradients involves the determination of other parameters than those in the internal calibration. We assume the latter has been performed to the specifications, so that the error in the MBW is below the required level.

The subscript s of '$\mathbf{y}_s$' refers to the static gravity field. It is here assumed that a correction is applied for the temporal part of the Earth's gravity field. The true values $\mathbf{y}_s$ are of course unknown, but we can compute approximate values from an existing global gravity field model. In order to compute the calibration gradients the position of the instrument needs to be known. The GPS receiver on board GOCE should enable accurate orbit determination, down to the centimetre level (Visser and van den IJssel 2000), which is accurate enough for this purpose.

Under the assumption that the longer wavelengths of such a global gravity field model are accurately determined at the time that GOCE flies, it is fair to expect that external calibration using global models could remove systematic long-wavelength errors from the gravity gradient time series. Hence, calibration parameters $\lambda, \mathbf{\Delta y}, \mathbf{y}'$ and a_k, b_k can be estimated using measured gradients $\underline{\mathbf{y}}(t)$ and calibration gradients $\mathbf{y}_s(t)$. For low frequencies, below the MBW, the latter have a smaller error than the former. If it is assumed that the gravity gradient scale factors do not depend on frequency, then they are also valid in and above the MBW, even though they have been mainly determined by the long-wavelength part of the gravity field signal, since the power at 0, 1 and 2 cpr dominates the signal.

The (propagated) error of the global gravity model used to compute the calibration gradients is not taken into account here. One way to do so is to introduce the calibration gradients themselves as observations with their corresponding propagated error, and to estimate calibration parameters together with calibrated gradients using a model of condition equations. A major problem of such an approach is that the system of equations becomes very large due to the error correlation. Bouman and Koop (2003) used condition equations and neglected all error correlations, and their results are similar to the results presented in this paper for $\mathbf{V}_{ZZ}$ (second radial derivative of the gravitational potential).

We remark that an alternative method for external calibration could be to estimate calibration parameters together with the gravity field parameters in the data reduction step (gravity field inversion process). This method is not further discussed here (see e.g. Reigber et al. 2003).

3 Calibration of GOCE SGG data using global gravity field models

In this section we will use global gravity field models to determine the calibration parameters of the model in Eq. (1) and calibrated gradients. We must rely on simulated measurements because there are no real SGG data available yet. In Sects. 3.1–3.3 we will describe the simulated data set, and we will focus on the determination of some or all of the unknowns in Eq. (1) and on the success of the external calibration, in terms of gravity gradient error reduction.

3.1 Description of the test measurement data set

A GOCE-like orbit was generated using the EGM96 model (Lemoine et al. 1998) truncated at spherical harmonic degree and order $L = 300$. The orbit has an inclination of 96.6°, a height of approximately 250 km, and an eccentricity of 10^{-3}. Gravity gradients were generated using the same global gravity field model (EGM96) along the orbit for a mission length of 30 days and a sampling interval of 5 s. Thus the number of data points is approximately half a million. The three main gradient observables are $\mathbf{V}_{XX}, \mathbf{V}_{YY}$ and $\mathbf{V}_{ZZ}$ in the LORF. (In the Appendix, V_{XX} etc. are the gravity gradient tensor components at one point. Here $\mathbf{V}_{XX}$ etc. are time series of gravity gradients.)

Realistic errors have been generated with the SRON SGG instrument simulator (see SID 2000). The simulated errors, which are the remaining errors after internal calibration, were added to the gravity gradients and the resulting erroneous gradients serve as our observations that need to be externally calibrated.

3.2 Calibration of gravity gradients without errors

In Sect. 3.3 the calibration of the gravity gradients with simulated errors is discussed. Prior to this, however, we will set benchmarks of existing and near future global gravity field models for calibration. True gravity gradients $\underline{\mathbf{y}}(t)$, generated with EGM96 complete up to degree and order $L = 300$, were calibrated using three different global gravity field models. In ESA (1999) it is suggested to determine the gradiometer's absolute scale factors using the accurate knowledge of the J_2 gravity gradient variations and the coupling between the central term (or J_0) and the radial orbit variations [case (1)]. One disadvantage of using just J_0 and J_2 is that the gravity gradient omission error may be large. We therefore also considered OSU91A (Rapp et al. 1991) complete up to degree and order $L = 300$ [case (2)], which gives an indication of today's achievable accuracy (conservative estimate). Finally, a GRACE-like global gravity field model is considered. With the launch of GRACE in March 2002, it was expected that the Earth's long-wavelength gravity field could accurately be determined (Tapley and Reigber 1999). The EGM96 model complete up to degree and order $L = 120$ was used as a GRACE gravity field model [case (3)]. Despite the omission error, the calibration results are likely to be optimistic in this case, since the spherical harmonic coefficients up to degree and order $L = 120$ are without error.

Table 1. Scale factor errors $|1-\lambda|$ when scale factor and bias are estimated

	V_{XX}	V_{YY}	V_{ZZ}
(1) GM, J_2	$2 \cdot 10^{-4}$	$5 \cdot 10^{-5}$	$2 \cdot 10^{-4}$
(2) OSU91A	$2 \cdot 10^{-7}$	$2 \cdot 10^{-5}$	$1 \cdot 10^{-5}$
(3) GRACE	$7 \cdot 10^{-8}$	$9 \cdot 10^{-6}$	$4 \cdot 10^{-6}$

Calibration gravity gradients $\mathbf{y}_s(t)$ were computed, using models (1)–(3), at the same orbit points at which the true gravity gradients were simulated. Next, scale factors λ and biases for the three diagonal gravity gradients were determined in an iterative least squares (LS) adjustment using a linearised version of Eq. (1). Ideally, the scale factors so determined are equal to one, while the biases could compensate for the (small) mean difference between the true gradients and the calibration gradients.

Table 1 lists the scale factor errors $|1-\lambda|$ for the three types of gravity gradients for the three cases. These errors are 10^{-4} using J_0 and J_2 to compute the calibration gradients. For the OSU91A case the scale factor error for the $\mathbf{V}_{XX}$ component is reduced by three orders of magnitude to 10^{-7} and it is reduced to 10^{-5} for $\mathbf{V}_{YY}$ and $\mathbf{V}_{ZZ}$, which are reductions by factors of 2.5 and 20 respectively. The large reduction for the $\mathbf{V}_{XX}$ gradient may be due to its sensitivity to the lumped zonal coefficients that are accurately known, whereas $\mathbf{V}_{YY}$, for example, is less sensitive to the zonals. The GRACE case shows that an improved knowledge of the long-wavelength gravity field decreases the scale factor errors by a factor of two to three as compared to calibration with OSU91A.

It should be noted that the bias and scale factor are heavily correlated (correlation of almost ± 1). The mean and root mean square (RMS) about the mean of the signals $\mathbf{V}_{XX}, \mathbf{V}_{YY}$ and $\mathbf{V}_{ZZ}$, for the current simulation, are (−1371 E, 5.6 E), (−1369 E, 4.5 E) and (2740 E, 10.1 E) respectively. Thus the signal RMS is small compared to the size of the signal. Therefore, a scale factor and a bias have almost the same effect and cannot be determined independently using only a global gravity field model for calibration.

3.3 Calibration of gravity gradients with errors

It can be concluded from the calibration of gravity gradients without errors that it seems better to determine gravity gradient scale factors using a *full* global gravity field model. Hence, in this section we will only use the OSU91A and GRACE gradients to calibrate the simulated gravity gradients with errors.

The 30-day time series of the $\mathbf{V}_{XX}$ errors (simulated − true) are shown in Fig. 1. There is a large mean error of −1.5 E, and the error RMS increases toward the end of the 30-day period. The latter is related to the increase of the radial orbit variation, which is also shown in Fig. 1. The height of the satellite above a reference sphere is shown. As the orbital height decreases, the signal, e.g. $\mathbf{V}_{ZZ}$, increases, and vice versa. Since the gradiometer is not perfect (for example, one accelerometer may be rotated with respect to its nominal position), a part of the $\mathbf{V}_{ZZ}$ signal may leak into the $\mathbf{V}_{XX}$ measurement. In the $\mathbf{V}_{XX}$ measurement, this leaked $\mathbf{V}_{ZZ}$ signal part contributes to the error. The gravity gradient errors and the signal are therefore correlated; see also the Appendix. Whereas the $\mathbf{V}_{ZZ}$ errors show a behaviour similar to the $\mathbf{V}_{XX}$ errors, the $\mathbf{V}_{YY}$ errors are slightly different. Because the satellite mainly rotates around the Y-axis, the error in the recovery of this rotation, from the measured accelerations, directly maps onto the $\mathbf{V}_{XX}$ and $\mathbf{V}_{ZZ}$ measurements, but not onto the $\mathbf{V}_{YY}$ measurements.

In Fig. 2 the PSD of the $\mathbf{V}_{XX}$ errors is shown. Clearly, the errors at 1, 2, 3 and 4 cpr are large (peaks between 10^{-4} and 10^{-3} Hz), and in addition the errors on the low frequencies between 0 and 1 cpr are large. The former are caused by the coupling between the error and the signal, which is large at 1 and 2 cpr due to the Earth's flattening and the orbital eccentricity, while the latter are due to the accelerometer instability for lower frequencies. The $\mathbf{V}_{ZZ}$ errors show similar behaviour, while the $\mathbf{V}_{YY}$ errors at 3 and 4 cpr are relatively small (not shown).

The calibration of Sect. 3.2 is repeated, but now for the gravity gradients with errors. The estimated calibration parameters are a scale factor, a bias and a trend for the total data set (30 days) for each of the three diagonal gradients. The errors of the calibrated $\mathbf{V}_{XX}$ and $\mathbf{V}_{YY}$ gradients are shown on the left in Fig. 3 (calibrated − true), while the error reductions with respect to the uncalibrated measurements are listed in Table 2. The mean error now is approximately zero, but systematic long-wavelength errors at 1, 2, ... cpr or at other frequencies cannot be removed. Estimating in addition Fourier coefficients for 1, 2, 3 and 4 cpr for $\mathbf{V}_{XX}, \mathbf{V}_{ZZ}$, and

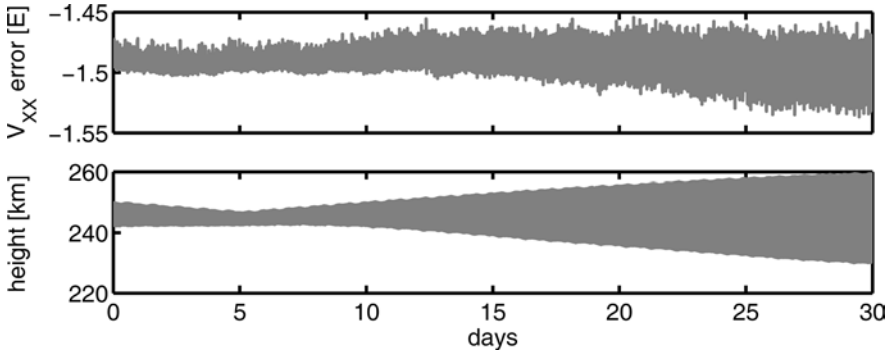

Fig. 1. Simulated $\mathbf{V}_{XX}$ gravity gradient errors before calibration (*top panel*) and the variation of the orbital height with respect to a reference sphere (*bottom panel*)

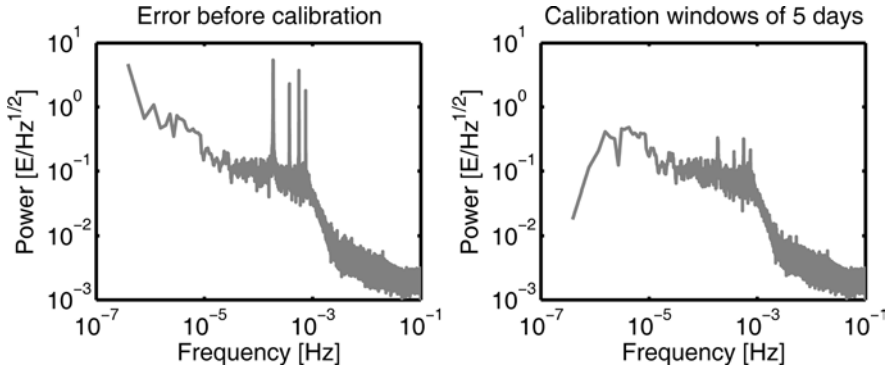

Fig. 2. PSD of $\mathbf{V}_{XX}$ gravity gradient errors before (external) calibration (*left panel*). Errors after calibration with OSU91A estimating scale factor, bias, trend and up to 4-cpr Fourier coefficients for each calibration window of 5 days (*right panel*). For display clarity the PSD's have been smoothed

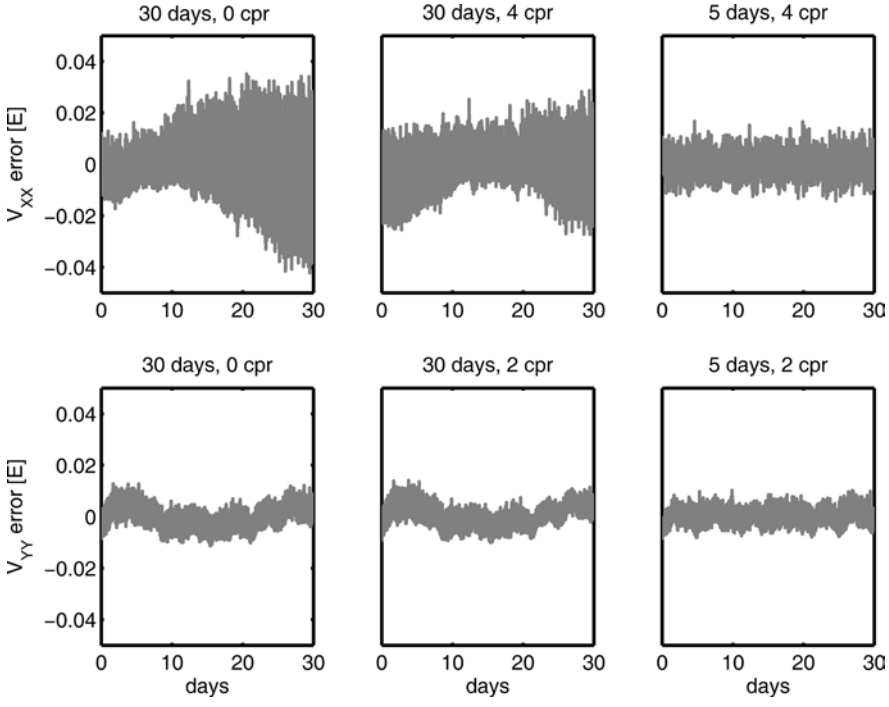

Fig. 3. Time series of gravity gradient errors after calibration. The title of each sub-panel indicates the calibration window length as well as the maximum frequency (in cpr) of the Fourier coefficients to be estimated. Other calibration parameters are scale factor, bias and trend for each window

Table 2. Standard deviation of the errors after calibration with OSU91A. The numbers give the fraction with respect to the standard deviation of the errors before calibration. The numbers for calibration with GRACE gradients are given in parentheses. Besides a scale factor, bias and trend, $\boldsymbol{V}_{XX}$ and $\boldsymbol{V}_{ZZ}$ are calibrated with 4-cpr coefficients (except for the 0-cpr case), while $\boldsymbol{V}_{YY}$ is calibrated with 2-cpr coefficients (except for the 0 cpr case)

Window	cpr	$\boldsymbol{V}_{XX}$	$\boldsymbol{V}_{YY}$	$\boldsymbol{V}_{ZZ}$
1×30 days	0	0.87 (0.87)	0.85 (0.84)	0.74 (0.74)
1×30 days	2/4	0.64 (0.64)	0.84 (0.80)	0.54 (0.53)
6×5 days	2/4	0.29 (0.29)	0.54 (0.42)	0.32 (0.27)
30×1 day	2/4	0.25 (0.24)	0.68 (0.30)	0.37 (0.23)

for 1 and 2 cpr for $\mathbf{V}_{YY}$ removes part of the systematic effect at these frequencies and further reduces the total error (see Table 2, third row). Calibration with the GRACE model is only marginally better than calibration with OSU91A.

Although the gravity gradient errors have been reduced, we are now confronted with at least two limitations of our model Eq. (1). The first is that long wavelengths between 0 and 1 cpr are largely uncalibrated, only a scale factor and a trend have effect at these low frequencies. Second, as explained above, the gravity gradient errors are correlated with the orbital height variation, which changes slowly but significantly with time. Therefore, the signal and the errors at 1, 2, ... cpr vary in time as well, and the estimated Fourier coefficients are not representative of the whole 30-day period. One way to deal with these problems is to divide the calibration period into shorter calibration windows and to estimate new calibration parameters for each observation window. If the window is small enough, then the estimated Fourier coefficients are representative of this window. In addition, this windowing will remove part of the long-wavelength errors below 1 cpr: if calibration gradients are very accurate at the long wavelengths, then the window size determines the longest possible wavelength of the errors in the calibrated gradients.

The total observation period of 30 days has been divided into six windows of 5 days. For each of these

windows we determined the full set of calibration parameters, that is, scale factor, bias, trend and up to 2-cpr Fourier coefficients for $\mathbf{V}_{YY}$ and up to 4-cpr Fourier coefficients for the other two gradients. Results for $\mathbf{V}_{XX}$ are shown in Fig. 2, while Table 2 summarizes the reduction of the standard deviation of the errors with respect to the original uncalibrated gradients. As expected, the long-wavelength errors are reduced using shorter calibration periods. A period of 5 days, for example, corresponds to 2.3×10^{-6} Hz, and it is clear from Fig. 2 (right panel) that the errors below this frequency have indeed become smaller. Furthermore, the errors at 1–4 cpr have been largely reduced. Calibration with the GRACE model is better than calibration with OSU91A, except for $\mathbf{V}_{XX}$. Again, the latter may be due to our accurate knowledge of the zonal harmonics to which $\mathbf{V}_{XX}$ is particularly sensitive.

As mentioned above, model Eq. (1) gains validity for shorter calibration windows, but for a shorter calibration window fewer observations are used in the determination of the calibration parameters. Therefore, the calibration window cannot be made arbitrarily small. The shorter the calibration window, the more accurate the calibration gradients must be, and the better long-wavelength errors can be removed from the GOCE gradients. Conversely, the longer the calibration window, the more the errors in the calibration gradients are averaged, which improves the calibration results, be it that long-wavelength errors remain. This is illustrated by Table 2. A calibration period of 1 day improves the results for $\mathbf{V}_{XX}$, but the errors for $\mathbf{V}_{YY}$ and $\mathbf{V}_{ZZ}$ become larger. Calibration with the GRACE model is significantly better than calibration with OSU91A, except for $\mathbf{V}_{XX}$. The latter results show that, if a very accurate long-wavelength global gravity field model is available, the error standard deviation of the calibrated gradients can be reduced to between one-third and one-quarter of the original uncalibrated gravity gradient error. Note that although the error reduction with respect to the original uncalibrated gradients for $\mathbf{V}_{YY}$ is not as much as for the other two diagonal components, the total error for $\mathbf{V}_{YY}$ is small. The limited accuracy with which we can derive the Y-rotation will only contaminate $\mathbf{V}_{XX}$ and $\mathbf{V}_{ZZ}$, which yields smaller $\mathbf{V}_{YY}$ errors (see Table 3).

The mean of the error of the calibrated gradients is very small, but not equal to zero. This is caused by the difference in the mean between OSU91A and EGM96 for $\mathbf{V}_{XX}$ and $\mathbf{V}_{YY}$. Maybe this small mean error can be reduced using the accurate knowledge of the GOCE orbit after precise orbit determination (POD). As a rule of thumb, an orbit error of 10 cm in the radial direction yields a gradient error of 0.1 mE due to the change in GM/r^3. Since the POD is expected to give an average orbit error at centimetre level, it is may be possible to decrease the mean of the gravity gradient errors to 0.1 mE or less. This is, however, an open issue.

Table 3. Standard deviation and mean of the errors before and after calibration with OSU91A

	V_{XX}	V_{YY}	V_{ZZ}
Standard deviation			
Before calibration	11.2 mE	4.4 mE	12.0 mE
6×5 days	3.2 mE	2.4 mE	3.9 mE
Mean			
Before calibration	−1.49 E	−0.82 E	2.31 E
6×5 days	−0.2 mE	0.2 mE	0.0 mE

One way to determine the calibration window length in practice is to use the a priori error models of the measured gradients and the calibration gradients. The error model of the latter is obtained by propagating the error model of the spherical harmonic coefficients to the respective gravity gradients (this is the commission error). Assuming that the calibration gradients are more accurate at longer wavelengths than the measured gravity gradients, while the latter are more accurate at shorter wavelengths, there will be a cross-over frequency where they are equally accurate. It probably does not make sense to use window lengths shorter than the window length corresponding to that frequency, which may be different for different gradients. If the omission error of the calibration model is relatively large, then this should be added to the commission error. In addition, if Fourier coefficients are to be estimated, the minimum window length should be at least a couple of revolutions. Alternatively, we could estimate, in a sensitivity analysis, the accuracy of the calibration parameters for different window lengths. The shorter the calibration window, the less accurate the calibration parameters for that window will be. We should decide by some criterion what calibration parameter accuracy is acceptable, which will determine the window length.

A possible drawback of estimating new calibration parameters for each window is that the calibrated gravity gradients may show discontinuities going from one window to another. A discontinuity would indicate that the long-wavelength error of the calibration gradients is large compared to the measurement noise on the GOCE gradients. Therefore, if the global gravity field model, used to compute the calibration gradients, is accurate at long wavelengths and/or the window length is not too small, then it is not expected that discontinuities will appear. Nevertheless, we could try to avoid discontinuities by changing the calibration model Eq. (1). A simple idea is to estimated scale factor, bias and trend for the whole calibration period and new Fourier coefficients for each window, which will reduce the discontinuity risk. The Fourier terms are anyway the parameters that are expected to vary in time, while the others are expected to be constant for longer periods. Another idea is to replace the bias and trend estimate by a spline function, which guarantees continuity, be it that new Fourier coefficients for each window and/or a scale factor could violate this. An even more drastic change with respect to our original calibration model is to use a different analysis technique, for example wavelets. This is, however, outside the scope of this paper.

4 Calibration of GOCE SGG data using terrestrial gravity data

In addition to calibration of GOCE SGG data using global gravity field models, it is also possible to combine a global model with terrestrial gravity data in a regional approach. Since the long-wavelength gravity field is not well represented by the local data, the contribution of a global gravity field model was subtracted from the local terrestrial data, which removes most of the long-wavelength part. Furthermore, this makes the local data statistically more homogeneous, which is an advantage for LSC (Moritz 1980). Later on, the removed effects can be restored.

In this study, only one area is used. It is therefore not possible to estimate all parameters of Eq. (1) independently. In particular, the errors of the measured gravity gradients at long wavelengths, e.g. 1 and 2 cpr, appear to be constant in a limited region. Hence, when we estimate a bias, it is in effect a 'lumped' bias comprising the effects of scale factor, bias and errors at long wavelengths. This situation may improve when several regional calibration areas are used. It should be noted that the SGG measurements are calibrated over a wide range of values, because we start with the absolute values, which are however converted to anomalies in the remove–restore framework.

The external calibration of the GOCE gradiometer measurements using terrestrial data has been studied by Arabelos and Tscherning (1998) using real data for an area in Western Canada, but east of the Rocky Mountains, where the gravity field is very smooth. Using LSC, gravity gradient data were generated at satellite altitude along simple north-going or east-going tracks. First a bias and second a tilt were added to the data, and it was demonstrated how these quantities could be recovered using LSC with simultaneous bias and/or tilt parameter estimation by combining the ground data and the satellite data. Meanwhile the GOCE orbit has been fixed (ESA 1999), so that now realistic orbits can be generated.

The original investigation used, as mentioned, data generated and later recovered by LSC. We wanted to design a slightly more 'difficult' test by using data generated from a spherical harmonic model (EGM96) both at ground and at satellite level. A total of 10201 gravity values were generated from EGM96 in a $0.1 \times 0.15°$ grid in the area bounded by 35–45°N, 5–20°E, i.e. including 35°N (the Alps), and therefore having a much larger gravity variance than the one used in the Canadian plains (see Fig. 4). In addition, from the data set described in Sect. 3.1, GOCE orbit points were selected in an inner area: 37–43°N, 8–17°E, which amounts to a total of 532 points with the second-order radial derivative $\mathbf{V}_{ZZ}$ (the gradients without errors were used). The subsequent computations are simplified by rotating the Z-axis such that it becomes exactly radial. Note that due to the small eccentricity of the GOCE orbit the differences between the LORF and the radial frame are small. Instead of $\mathbf{V}_{ZZ}$ we could have used any other component of the SGG measurements, which furthermore could have been given in the instrument frame (Tscherning 1976, 1993).

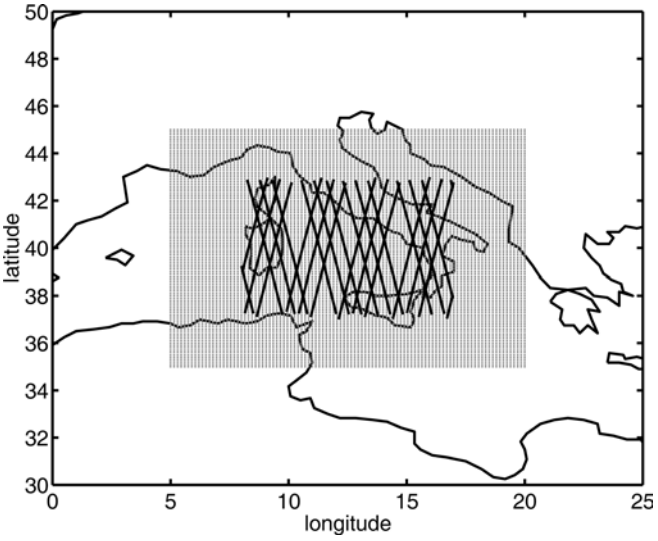

Fig. 4. Location of grid with gravity anomalies (*grey*) and the GOCE ground tracks (*black*)

Table 4. The different Δg and T_{ZZ} data sets

Set	Model	No. points	Quantity
GA	EGM96 – OSU91A ($L = 72$)	10 201	Δg
OA	EGM96 – OSU91A ($L = 72$)	532	T_{ZZ}
OL	OA from GA with LSC	532	T_{ZZ}

From the two sets of values, gravity and gravity gradients, the contribution of OSU91A to degree 72 was subtracted, which is equivalent to using the OSU91A coefficients as observed quantities in LSC, where the errors of the coefficients are taken into account by the covariance function model (see Knudsen 1987). The two resulting sets will be called GA and OA (see also Table 4). We are now dealing with gravity anomalies Δg and gravity gradient anomalies $\mathbf{T}_{ZZ}$ instead of full gravity values and gravity gradients. Hence gravity gradients are here denoted as $\mathbf{T}_{ZZ}$ instead of $\mathbf{V}_{ZZ}$. The gravity variance of set GA was large: 1349 mGal^2. The empirical covariance function was estimated for the area, and an analytical model (Tscherning–Rapp model) was fitted to the estimated values using the program COVFIT (Knudsen 1987). From the analytical model the signal RMS of $\mathbf{T}_{ZZ}$ was found to be 0.09 E. For the inner area the signal was found to have a mean of 0.0217 E and a signal RMS of 0.0988 E.

In addition, $\mathbf{T}_{ZZ}$ was predicted from the ground gravity, set GA, using LSC. This will be called set OL. The gravity data had been assigned an error of 1 mGal in the LSC normal equations, but no noise was added to the data, so that it was possible to verify the consistency of the two data sets OA and OL. The results for the differences are summarized in the second column of Table 5. There is a small bias, but otherwise LSC predicts the $\mathbf{T}_{ZZ}$ values correctly. Although this bias is at an

Table 5. Differences between T_{ZZ} values directly from EGM96 and LSC predicted values from ground data generated with EGM96 (second column). Bias recovery results using LSC with parameter (bias) estimation (third column)

	Differences	Bias recovery
Mean	−5.7 mE	−5.8 mE
Standard deviation	1.7 mE	0.5 mE
LSC error estimate	3 mE	1 mE
Maximum	1.8 mE	−4.7 mE
Minimum	−10.6 mE	−6.5 mE

acceptable level, further improvements are foreseen by abandoning the spherical approximation and possibly by expanding the area size. The larger the outer region with gravity data, the more reliable the upward continuation will be, which reduces the bias.

The LSC error estimates of the predicted gravity gradients were generally of the order of 3 mE. Consequently, if we are able to upward continue the gravity data and determine the gravity gradients with an error of this magnitude, a simple comparison with the observations may reveal contingent scale factors, biases or tilts (drifts). For this purpose we could use a calibration model such as Eq. (1) and estimate, for example, calibration parameters per track. The procedure therefore consists of two steps. First, gravity gradients are predicted at satellite level using LSC: second, calibration parameters and calibrated gradients may be determined.

Instead of the two-step procedure described in the previous paragraph, *LSC with parameters* (Moritz 1980) may be used to estimate such parameters (scale factors, biases, etc.) in one step by combining ground and satellite data, the advantage being that the error due to the ground data distribution may be calculated. The error of such estimates will depend on how many points on a track are inside a calibration area. We therefore extracted from the data set all tracks for which at least 18 points were located within the area. In total, 28 tracks with 532 observations were used. The ground tracks of most of the tracks crossed each other. The bias was determined using the 'true' gradients (set OA) in combination with the ground data. The calculation of error estimates of the biases resulted in a standard error of 1 mE. This is a very satisfactory result. The bias recovered is the one already seen when comparing observed and predicted gravity gradient values, i.e. −5.8 mE, (see Table 5). It is slightly different for the different tracks, their standard deviation is 0.5 mE.

The results are in good agreement with the earlier results from the Canadian plains, and it is shown that external calibration is possible in areas with larger gravity variations, the problem being that in such areas we seldom have data of the same high quality as found on the Canadian plains. However, airborne gravimetry now has the capability of measuring gravity at the 1 mGal level. It might be worthwhile to use airborne gravity data for the establishment of calibration data in areas with a large gravity signal.

The above simulations show that a bias is introduced in the GOCE calibration gradients that are computed using LSC in spherical approximation and terrestrial gravity data in a limited area. The bias is at the 1–10-mE level (assuming that the terrestrial gravity data themselves do not suffer from an offset). A bias in the GOCE gravity gradients can therefore be recovered up to this accuracy level. If the bias, introduced by the spherical approximation and/or upward continuation, could be reduced using no approximation or larger areas with ground data, then the recovery of the bias in the GOCE gravity gradient data would be better.

Alternatively, the above results may be used to compute a priori the bias introduced by the spherical approximation and/or the upward continuation. If this 'model' bias is taken into account, then the second part of the simulations show that a bias recovery is very possible with LSC. If this is done, the zero bias in set OA is found to be −0.1 mE with a standard deviation of 0.5 mE. A prerequisite is, however, that the a priori gravity model which is used to compute a priori the 'model' bias is very accurate. Although it was not possible to estimate the calibration parameters of Eq. (1) independently, for we used only one area with terrestrial data, our results show that it may be possible to compute gravity gradients from terrestrial data for validation purposes.

5 Calibration of the CM accelerations

In the preceding two sections the external calibration of the GOCE gravity gradients was discussed. The gravity gradients are derived from the DM accelerations. In this section we will explore the possible calibration of the CM accelerations. With externally calibrated CM accelerations it may be possible to improve the separation of the gravitational and remaining non-gravitational forces, which is necessary for both POD (precise orbit determination) and gravity field determination.

In principle, the GPS receiver provides the information for deriving the orbit of the GOCE satellite, which is the integrated effect of all forces driving its motion. The following relation can be derived for the acceleration of GOCE:

$$\ddot{\mathbf{x}} = \mathbf{a}_{cf} + \mathbf{a}_{l} + \mathbf{a}_{\text{rem}} \tag{2}$$

where $\mathbf{x}$ denotes the 3-D position of the satellite in an Earth-centred pseudo-inertial reference frame and $\ddot{\mathbf{x}}$ its second-order time derivative (acceleration). The acceleration

$$\mathbf{a}_{cf} = \mathbf{a}_{\text{eg}} + \mathbf{a}_{\text{3rd}} + \mathbf{a}_{\text{tid}} \tag{3}$$

represents the effect of the most important contributing gravitational forces $\mathbf{a}_{\text{eg}}$ (Earth's gravity field), $\mathbf{a}_{\text{3rd}}$ (third bodies, such as the Moon, Sun and planets) and $\mathbf{a}_{\text{tid}}$ (solid Earth and ocean tidal forces). The linear acceleration

$$\mathbf{a}_{l} = \mathbf{a}_{\text{drag}} + \mathbf{a}_{\text{sol}} + \mathbf{a}_{\text{DFC}} \tag{4}$$

represents the effect of the most important non-gravitational forces $\mathbf{a}_{\text{drag}}$ (atmospheric drag), $\mathbf{a}_{\text{sol}}$ (solar radiation pressure) and $\mathbf{a}_{\text{DFC}}$ (control forces from the GOCE DFC system). In the following we will neglect the remaining accelerations $\mathbf{a}_{\text{rem}}$ from Eq. (2).

5.1 CM calibration principle

In principle the CM of the gradiometer measures the linear accelerations $\mathbf{a}_l$, [see Eq. (A3)]. Two possibilities can be distinguished for checking these observations:

(1) compare $\mathbf{a}_l$ with a priori models for the atmospheric drag ($\mathbf{a}_{\text{drag}}$), solar radiation ($\mathbf{a}_{\text{sol}}$) and accelerations modelled from the information from DFC-telemetry ($\mathbf{a}_{\text{DFC}}$);
(2) use a priori gravitational force models to derive $\mathbf{a}_{cf}$ and reduce the GPS-based acceleration $\ddot{\mathbf{x}}$ to the linear acceleration $\mathbf{a}_l$.

Since the current knowledge on atmospheric drag models is still relatively poor, especially at low altitudes as for GOCE, the first possibility will not be further elaborated on here. For the second possibility, the ideal situation would be that $\mathbf{x}$ and indirectly $\ddot{\mathbf{x}}$ could be derived perfectly from the GPS observations ($\ddot{\mathbf{x}} = \ddot{\mathbf{x}}_{\text{GPS}}$) and that the gravitational force models $\mathbf{a}_{cf} = \mathbf{a}_{cf,\text{mod}}$ are known perfectly. In that case the linear accelerations could be derived without error [using Eq. (2)] as

$$\mathbf{a}_{l,\text{GPS}} = \ddot{\mathbf{x}}_{\text{GPS}} - \mathbf{a}_{cf,\text{mod}} \tag{5}$$

They could then be compared with the measured linear accelerations $\mathbf{a}_{l,\text{CM}}$ from the gradiometer CM when transformed to the same reference frame.

In reality, the position of GOCE can be only reconstituted to a certain precision (so that $\mathbf{x}$ and $\ddot{\mathbf{x}}$ will not be known perfectly), introducing an error

$$\delta\ddot{\mathbf{x}}_{\text{GPS}} := \ddot{\mathbf{x}} - \ddot{\mathbf{x}}_{\text{GPS}} \tag{6}$$

Also, all gravitational force models are only accurate to a certain degree, introducing an error

$$\delta\mathbf{a}_{cf} := \mathbf{a}_{cf} - \mathbf{a}_{cf,\text{mod}} = \delta\mathbf{a}_{\text{eg}} + \delta\mathbf{a}_{\text{3rd}} + \delta\mathbf{a}_{\text{tid}} \tag{7}$$

Furthermore, the transformation of the linear accelerations to the relevant frame to enable comparison can only be done to a certain accuracy, introducing an error $\delta\mathbf{a}_{\text{transf}}$. Considering all these errors, the estimated GPS-based linear acceleration is [using Eq. (2)]

$$\mathbf{a}_{l,\text{GPS}} = \mathbf{a}_l + \delta\mathbf{a}_{\text{transf}} - \delta\ddot{\mathbf{x}}_{\text{GPS}} + \delta\mathbf{a}_{cf} \tag{8}$$

It has to be assessed whether, possibly only for certain spectral bands

$$\delta\mathbf{a}_l := \mathbf{a}_{l,\text{GPS}} - \mathbf{a}_l \tag{9}$$

is below the accelerometer observation noise level.

5.2 Simulation

To assess whether the error Eq. (9) is below the noise level the effect of aliasing of one dynamic model error, namely the uncertainty of the gravity field model ($\delta\mathbf{a}_{\text{eg}}$), has been assessed. The most important error source in modelling the orbit and accelerations of a very-low-flying satellite like GOCE is the uncertainty of existing gravity field models. In order to simulate a realistic gravity field model error, the differences between two relatively recent gravity field models, EGM96 and JGM3 (Tapley et al. 1996), were taken, where EGM96 is supposed to represent the real world and JGM3 the reference model. These two models are within each other's calibrated error bounds, so that the differences indeed represent realistic gravity field model errors, assuming that the calibration was done correctly.

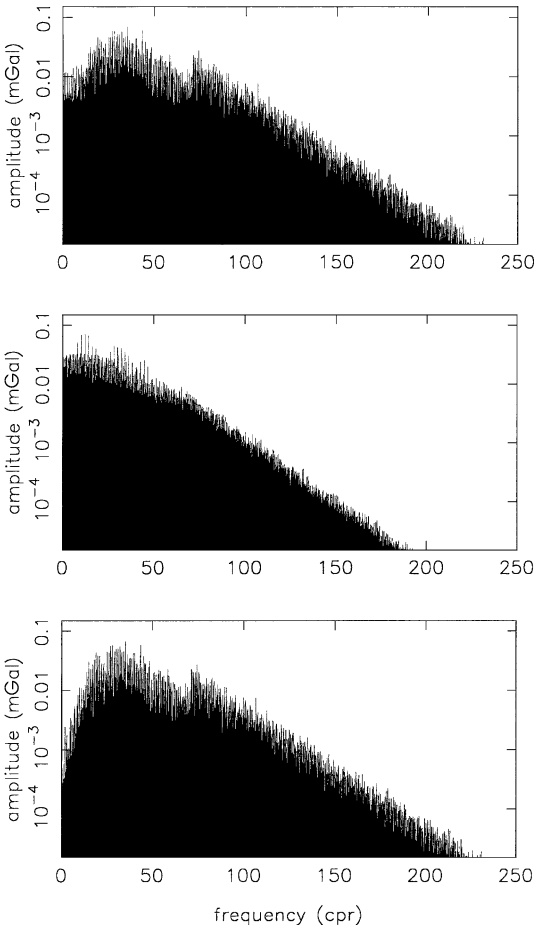

Fig. 5. Radial (*top*), along-track (*middle*) and cross-track (*bottom*) accelerations due to JGM3-EGM96 model differences for a GOCE-like orbit

First, the EGM96 and JGM3 coefficient differences were propagated to an amplitude spectrum of acceleration differences along a GOCE-like orbit. As an example, the accelerations caused by these differences for a satellite flying at 250 km altitude with an orbit inclination of 96° are displayed in Fig. 5. The RMS of the accelerations is equal to 0.40, 0.46 and 0.37 mGal (1 mGal = 10^{-5} m/s^2) for the radial, along-track and cross-track direction, respectively. These numbers are significantly above the foreseen accuracy level of the accelerometer observations to be derived from the CM of the gradiometer (specified in ESA 1999).

Table 6. Estimated constant accelerations obtained from simulated GPS-based precise orbit determinations for GOCE in the presence of JGM3/EGM96 gravity field model differences (values in mGal)

Arc length (rev)	Along-track	Cross-track	Radial
1	0.0308	0.0657	0.0131
2	−0.0120	0.0244	−0.0663
3	−0.0037	0.0359	−0.0725
4	−0.0003	−0.0035	−0.0792
5	0.0009	−0.0070	−0.0020
6	−0.0001	−0.0246	0.1062

Second, a precise orbit determination experiment was conducted for a GOCE-type orbit based on simulated error-free GPS observations. The simulation approach is based on error-free double differences, where use is made of a network of 24 ground stations. The approach is similar to those described in detail in ESA (2000), SID (2000) and Visser van den IJssel (2000). The real-world gravity field is described by the EGM96 model, truncated at degree and order 70. One set of average radial, along-track and cross-track GOCE accelerations is estimated for one orbital arc from the GPS observations using the JGM3 model as reference model. Different orbital arc lengths have been selected, ranging from 1 to 6 revolutions. This approach enables us to quantify the aliasing of EGM96/JGM3 model differences in accelerations that are estimated from GPS observations in a POD environment as a function of the averaging interval, in this case equal to the orbital arc length.

The results displayed in Table 6 show that the aliasing of gravity field model error is very serious, even for averaging intervals up to six orbital revolutions (about 9 hours): although the along-track acceleration has a value of −0.0001 mGal, the accelerations in the other two directions have much higher values, the cross-track acceleration even being as large as 0.1 mGal. In fact, the obtained values seem to depend in a rather random fashion on the orbital arc length. Based on these results, it may be concluded that it will be very difficult to calibrate the CM accelerations to the required accuracy level when using GPS observations. Moreover, it has to be noted that the only error present was the gravity field model error.

However, it may be argued that at the very low frequencies the drag compensation will probably not be complete and a relatively large long-period signal may remain that is above the gravity field model error and thus visible by the common mode of the gradiometer. Furthermore, at the time GOCE flies, our gravity field knowledge will certainly be improved, especially at the long wavelengths, as a result of the CHAMP and GRACE missions. The risk of circular reasoning arises, however, as CHAMP and GRACE will also make use of accelerometer and GPS observations. In fact, the first CHAMP-based gravity field models are based on a simultaneous estimation of accelerometer and gravity field unknowns (Reigber et al. 2001). Although it seems that this approach leads to significant improvements in gravity field modelling, the separation of gravitational and non-gravitational accelerations cannot be guaranteed.

6 Conclusions

A full calibration setup for GOCE data includes a preflight on-ground test, a repeated in-flight internal calibration procedure and post-mission external calibration. In the external calibration step, GOCE data are compared with external data sources, and corrections are computed. If in the on-ground and internal calibration steps the CM and DM accelerometer scale factors are accurately determined, then the absolute accelerometer scale factors are accurately determined as well. However, this does not immediately imply that the gravity gradient scale factors are known accurately. There are error sources for which the on-ground and internal calibration are insensitive. In addition, the requirements for the internal calibration are such that in the MBW maximum sensitivity is obtained. Large systematic errors below the MBW could therefore go undetected. It is desirable to correct the gravity gradients for such errors because the gradients are an important end product in themselves. External calibration is needed to correct for the remaining errors.

Depending on the choice of the (external) calibration data, several calibration methods can be distinguished, for example using ground-based gravity data or global gravity field models. The latter external data source offers the possibility to correct for systematic errors in the GOCE SGG data in the longer wavelength part below the MBW. If the gravity gradient scale factors are constant for all frequencies, then our calibration method also calibrates inside the MBW, although the scale factors are mainly determined by the long-wavelength gravity field signal. The current simulations show that the error RMS after the internal calibration can be reduced by a factor of two to three, depending on the particular gravity gradient. Today's global gravity field models have sufficient long-wavelength accuracy for calibration purposes, but in the near future CHAMP and GRACE models may improve the calibration results.

The determination of gravity gradient scale factors using just the knowledge of the central term and the flattening of the Earth's gravity field is not accurate enough. Instead, it is necessary to use higher-degree and-order terms of the spherical harmonic expansion as well. Moreover, if systematic errors at 1–4 cpr are to be removed, then GM and J_2 cannot be used. For that purpose the use of higher-degree global gravity field models is recommended.

Due to the variations in orbital height during the mission, the frequency characteristics of some of the systematic errors, which depend on the signal, are not constant in time. External calibration of the gravity gradients for the full 30-day period between successive internal calibrations is therefore not as good as external calibration for shorter time windows. How long these time windows should be depends on the

long-wavelength accuracy of the calibration model compared to the gravity gradients.

External calibration using terrestrial gravity in an LSC approach shows that currently bias determination is possible down to the 1–10 mE level. This lower limit may be reduced using a larger area with ground data and/or the actual positions of the points in space instead of a spherical approximation. While it may be difficult to calibrate the whole global gravity gradient data set with local data, it may be possible to use terrestrial data for validation purposes.

The possibilities of checking the CM observations with the SST data are strongly limited by the errors in the gravity force modelling. With the improved gravity field knowledge from CHAMP and GRACE, the calibration of the CM may become feasible.

Acknowledgments. The satellite orbit and the EGM96 gravity gradients were provided by Karl Heinz Ilk as part of simulation scenarios of Special Commission 7 in cooperation with Special Study Group 2.193 of the International Association of Geodesy, which is appreciated. Volker Hannen computed the simulated gravity gradient errors, which is also appreciated. The authors also acknowledge the use of `newmat`, a C++ matrix library developed by Robert Davies. The software can be downloaded from the Internet, and this matrix library supported part of the computations. Finally, three anonymous reviewers whose remarks helped to improve the manuscript are thanked.

Appendix

From accelerations to gravity gradients

The GOCE gravity gradiometer consists of six accelerometers, which measure in three orthogonal directions (see Fig. A1) In this appendix we will describe the relation between the measured accelerations and common and differential mode accelerations, as well as how to derive gravity gradients from the DM accelerations. In addition, the different error sources and the on-ground and internal calibration are briefly discussed.

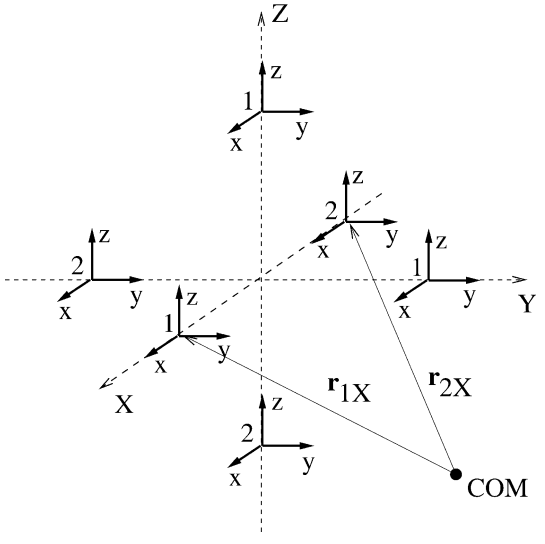

Fig. A1. The six accelerometers in the local orbital reference frame (LORF)

In each accelerometer a proof mass is electro-statically suspended and actively controlled at the centre of a cage by means of a feedback mechanism. The proof mass displacement relative to the electrodes is measured by capacitive sensors. The control voltages are representative of the accelerations of the proof mass relative to the cage. The relative acceleration $\mathbf{a}_{i\alpha}$ of the proof mass with respect to the cage is (ESA 1999; Cesare 2002) (i refers to the accelerometer number, α to the spatial direction, $i = 1, 2$ represents the two accelerometers on one gradiometer arm)

$$\mathbf{a}_{i\alpha} = \mathbf{a}_I + \ddot{\mathbf{r}}_{i\alpha} + 2\boldsymbol{\omega} \times \dot{\mathbf{r}}_{i\alpha} + \boldsymbol{\omega} \times \boldsymbol{\omega} \times \mathbf{r}_{i\alpha} + \dot{\boldsymbol{\omega}} \times \mathbf{r}_{i\alpha} - \mathbf{V}'' \mathbf{r}_{i\alpha} - \mathbf{s}_{i\alpha} - \mathbf{m}_{i\alpha}, i = 1, 2, \alpha = X, Y, Z \quad \text{(A1)}$$

where

- $\mathbf{a}_I$ is the linear acceleration of the satellite COM (centre of mass) due to all non-gravitational forces,
- $\mathbf{r}_{i\alpha}$ is the cage centre position vector relative to the satellite COM, with $\dot{\mathbf{r}}_{i\alpha}$ and $\ddot{\mathbf{r}}_{i\alpha}$ its time derivatives,
- $\boldsymbol{\omega}$ is the satellite angular velocity about the COM,
- $\mathbf{V}''$ is the gravity gradient tensor (second derivatives of the gravitational potential V);
- $\mathbf{s}_{i\alpha}$ is the acceleration of the proof mass due to other satellite masses (satellite self-gravity);
- $\mathbf{m}_{i\alpha}$ is the acceleration due to the coupling of the proof mass with the external magnetic field,
- $\boldsymbol{\omega} \times \boldsymbol{\omega} \times \mathbf{r}_{i\alpha}$ is the centrifugal acceleration due to the satellite angular rotation;
- $\dot{\boldsymbol{\omega}} \times \mathbf{r}_{i\alpha}$ is the acceleration due to the satellite angular acceleration,
- $2\boldsymbol{\omega} \times \dot{\mathbf{r}}_{i\alpha}$ is the Coriolis acceleration.

Since the cage is rigidly connected to the satellite, its velocity and acceleration with respect to the satellite COM are zero, $\dot{\mathbf{r}}_{i\alpha} = \ddot{\mathbf{r}}_{i\alpha} = 0$. If the accelerometer was in the COM then $\mathbf{r}_{i\alpha} = 0$ and the accelerometer would only sense the non-gravitational forces and the self-gravity and magnetic field forces. This is the GRACE concept where the non-gravitational forces are measured (Tapley and Reigber 1999).

A1 Common and differential mode

The common mode and differential mode accelerations are

$$\begin{pmatrix} \mathbf{a}_{c\alpha} \\ \mathbf{a}_{d\alpha} \end{pmatrix} := \frac{1}{2} \begin{pmatrix} \mathbf{a}_{1\alpha} + \mathbf{a}_{2\alpha} \\ \mathbf{a}_{1\alpha} - \mathbf{a}_{2\alpha} \end{pmatrix}, \quad \alpha = X, Y, Z \quad \text{(A2)}$$

Thus the 18 observed accelerations in $\mathbf{a}_{i\alpha}$ are transformed to three common mode accelerations $\mathbf{a}_{c\alpha}$ (= nine observations) and three differential mode accelerations $\mathbf{a}_{d\alpha}$ (= nine observations). If it is assumed that the centre of the frame formed by the six accelerometers is in the COM, and if the self-gravity and magnetic field forces are neglected, then

$$\begin{pmatrix} \mathbf{a}_{c\alpha} \\ \mathbf{a}_{d\alpha} \end{pmatrix} = \begin{pmatrix} \mathbf{a}_I \\ \boldsymbol{\omega} \times \boldsymbol{\omega} \times \mathbf{r}_{1\alpha} + \dot{\boldsymbol{\omega}} \times \mathbf{r}_{1\alpha} - \mathbf{V}'' \mathbf{r}_{1\alpha} \end{pmatrix} \quad \text{(A3)}$$

under the condition that $\mathbf{r}_{1\alpha} = -\mathbf{r}_{2\alpha}$, (see Cesare 2002). The common mode (CM) is therefore proportional to the non-gravitational forces and these measurements will be used in the drag-free control. The gravity gradient tensor is part of the differential mode (DM). The gravity gradients $\mathbf{V}''$ are not measured directly since the angular velocities and angular accelerations are projected onto the DM as well.

The angular accelerations $\dot{\omega}_\alpha$ can be obtained by taking certain linear DM combinations. For example:

$$\dot{\omega}_X = \frac{a_{dYz}}{l_Y} - \frac{a_{dZy}}{l_Z} \tag{A4}$$

where a_{dYz} is the differential acceleration along the Y-axis in the z-direction, and $l_\alpha := \|\mathbf{r}_{1\alpha} - \mathbf{r}_{2\alpha}\|$. Cyclic exchange of X, Y, Z and x, y, z gives the angular accelerations around the Y- and Z-axis. Integration of these accelerations, which also requires star-tracker observations, gives the angular velocities ω_α, with which the gravity gradient tensor components $\mathbf{V}''$ can be derived in combination with the DM accelerations (Cesare 2002). The diagonal tensor components are

$$V_{XX} = -2\frac{a_{dXx}}{l_X} - \omega_Y^2 - \omega_Z^2 \tag{A5}$$

and the off-diagonal components are

$$V_{XY} = -\frac{a_{dXy}}{l_X} - \frac{a_{dYx}}{l_Y} - \omega_X \omega_Y \tag{A6}$$

where again cyclic exchange in Eqs. (A5) and (A6) gives all nine tensor elements.

A2 Error contributions

The accelerometer measurements are not perfect, suffering from the following errors (for each of the six accelerometers).

1. The accelerometer is not aligned perfectly with the LORF; the pointing error of one accelerometer is small, which is described by the rotation matrix $\mathbf{R}_{i\alpha}$.
2. The three axes of the accelerometer are not perfectly orthogonal, which results in cross couplings between the accelerometer sensitivity axes; this is described by the symmetric coupling matrix $\mathbf{C}_{i\alpha}$.
3. The accelerations are measured with a scale factor, which is described by the diagonal matrix $\mathbf{S}_{i\alpha}$.
4. The proof mass is in a motionless condition somewhat away from the centre of the cage, which results in the diagonal quadratic factor matrix $\mathbf{Q}_{i\alpha}$.
5. The electronics readout chain introduces a bias $\mathbf{b}_{i\alpha}$ and noise $\underline{\mathbf{n}}_{i\alpha}$.

For the explicit formulation of these vectors and matrices we refer to Cesare (2002). The measured accelerations therefore are (underlined values are stochastic)

$$\underline{\mathbf{a}}_{i\alpha} = \mathbf{S}_{i\alpha}\mathbf{R}_{i\alpha}\mathbf{C}_{i\alpha}\mathbf{a}_{i\alpha} + \mathbf{Q}_{i\alpha}\mathbf{a}_{i\alpha}^2 + \mathbf{b}_{i\alpha} + \underline{\mathbf{n}}_{i\alpha} \tag{A7}$$

where the notation of the quadratic term means that each vector component is squared individually.

Because each accelerometer has two very sensitive axes and one less sensitive axis, three of the CM and DM accelerations will be more noisy than the other six. As a result of the gradiometer configuration, the diagonal gravity gradients V_{XX}, V_{YY}, and V_{ZZ} in particular have a high accuracy in the MBW.

A3 On-ground and internal calibration

Using Eqs. (A2) and (A7), the measured common and differential accelerations are (Willemenot 1999; Cesare 2002)

$$\begin{pmatrix} \underline{\mathbf{a}}_{c\alpha} \\ \underline{\mathbf{a}}_{d\alpha} \end{pmatrix} = (\mathbf{I} + \mathbf{M}_\alpha)\begin{pmatrix} \mathbf{a}_{c\alpha} \\ \mathbf{a}_{d\alpha} \end{pmatrix} + \frac{\mathbf{Q}_\alpha}{2}\begin{pmatrix} (\mathbf{a}_{c\alpha} + \mathbf{a}_{d\alpha})^2 \\ (\mathbf{a}_{c\alpha} - \mathbf{a}_{d\alpha})^2 \end{pmatrix} + \begin{pmatrix} \mathbf{b}_{c\alpha} \\ \mathbf{b}_{d\alpha} \end{pmatrix} + \begin{pmatrix} \underline{\mathbf{n}}_{c\alpha} \\ \underline{\mathbf{n}}_{d\alpha} \end{pmatrix} \tag{A8}$$

where the 6×6 matrices $\mathbf{M}_\alpha$ contain the common and differential scale factors, misalignments and couplings [coming from the evaluation and linearisation of the matrix product SRC in Eq. (A7)], the 6×6 matrices $\mathbf{Q}_\alpha$ contain the common and differential quadratic factors, and the last two terms are the common and differential bias and noise respectively.

It is the purpose of the *on-ground calibration* to measure the elements of $\mathbf{M}_\alpha$ with an error smaller than $10^{-2} - 10^{-4}$, depending on the element. The common scale factors, for example, are measured with an error of 10^{-2}. The quadratic factors of $\mathbf{Q}_\alpha$ are measured and physically adjusted to reduce them to as close to zero as possible. The determination of the elements of $\mathbf{M}_\alpha$ and $\mathbf{Q}_\alpha$ is repeated in orbit. This is the so-called *in-flight* or *internal calibration*, which should give more accurate results than the on-ground calibration. During the internal calibration the elements of the matrices $\mathbf{Q}_\alpha$ are measured and physically reduced below the specified limits by proof mass position adjustment. The outcomes of the internal calibration are estimates of the matrices $\mathbf{M}_\alpha$:

$$\underline{\hat{\mathbf{M}}}_\alpha = \mathbf{M}_\alpha + \delta\underline{\mathbf{M}}_\alpha \tag{A9}$$

where the differences $\delta\underline{\mathbf{M}}_\alpha$ are due to measurement errors and variations over time of the accelerometer scale factors, misalignments and couplings.

A4 Gravity gradient and CM/DM scale factors

In the internal calibration, among others, the common and differential accelerometer scale factors are determined. They are defined as

$$\begin{pmatrix} S_{c\alpha\eta} \\ S_{d\alpha\eta} \end{pmatrix} := \frac{1}{2}\begin{pmatrix} S_{1\alpha\eta} + S_{2\alpha\eta} \\ S_{1\alpha\eta} - S_{2\alpha\eta} \end{pmatrix},\ \alpha = X, Y, Z, \eta = x, y, z \tag{A10}$$

From the common and differential scale factors we can immediately derive the absolute accelerometer scale factors as

$$\begin{pmatrix} S_{1\alpha\eta} \\ S_{2\alpha\eta} \end{pmatrix} = \begin{pmatrix} S_{c\alpha\eta} + S_{d\alpha\eta} \\ S_{c\alpha\eta} - S_{d\alpha\eta} \end{pmatrix},\ \alpha = X, Y, Z, \eta = x, y, z \tag{A11}$$

Therefore, if the internal calibration yields accurate common and differential scale factors, then the accelerometer absolute scale factors are accurately determined as well.

However, this does not automatically imply that the absolute scale factors of the gravity gradients have been accurately determined. The non-orthogonality of the instrumental realisation of the $\{X, Y, Z\}$ frame and the mispositioning of the accelerometers only show up in the gravity gradients and not in the DM accelerations. Furthermore, the relation between the gravity gradients and DM accelerations is complicated and nonlinear, [see Eqs. (A3)–(A6)]. Also, the internal calibration is very accurate in the MBW, and less accurate below the MBW, where most of the gravity gradient signal is present. Consequently, the scale factor errors of both the DM accelerations and the gravity gradients may be small in the MBW, but the scale factor error for the total gravity gradient signal can be as large as, for example, 10^{-4}. With external calibration this error can be reduced, (see Sect. 3). Conversely, if we have accurately determined the gravity gradient absolute scale factors this does not mean that the differential scale factors are accurately determined.

References

Arabelos D, Tscherning C (1998) Calibration of satellite gradiometer data aided by ground gravity data. J Geod 72: 617–625

Bouman J, Koop R (2003) Calibration of GOCE SGG data combining terrestrial gravity data and global gravity field models. In: Tziavos I (ed) Gravity and Geoid 2002; 3rd Meeting of the IGGC, Ziti Editions, Thessaloniki, pp 275–280

Cesare S (2002) Performance requirements and budgets for the gradiometric mission. Issue 2 GO-TN-AI-0027, Preliminary Design Review, Alenia, Turin

European Space Agency (1999) Gravity Field and Steady-State Ocean Circulation Mission. Reports for mission selection; the four candidate earth explorer core missions. SP-1233(1), European Space Agency, Noordwijk

European Space Agency (2000) From Eötvös to mGal. Final report. European Space Agency, Noordwijk /ESTEC contract no. 13392/98/NL/GD

Knudsen P (1987) Estimation and modelling of the local empirical covariance function using gravity and satellite altimeter data. Bull Géod 61: 145–160

Koop R, Bouman J, Schrama E, Visser P (2002) Calibration and error assessment of GOCE data. In: Ádám J, Schwarz KP (eds) Vistas for geodesy in the new millenium. International Association of Geodesy Symposia Vol 125. Springer, Berlin Heidelberg New York, pp 167–174

Lemoine F, Kenyon S, Factor J, Trimmer R, Pavlis N, Chinn D, Cox C, Klosko S, Luthcke S, Torrence M, Wang Y, Williamson R, Pavlis E, Rapp R, Olson T (1998) The development of the joint NASA GSFC and the National Imagery and Mapping Agency (NIMA) geopotential model EGM96. TP 1998-206861, NASA Goddard Space Flight Center, Greenbelt

Moritz H (1980) Advanced physical geodesy. Herbert Wichmann, Karlsruhe

Rapp R, Wang Y, Pavlis N (1991) The Ohio State 1991 geopotential and sea surface topography harmonic coefficient models. Rep 410, Department of Geodetic Science and Surveying, The Ohio State University, Columbus

Reigber C, Schwintzer P, Koenig R, Neumayer KH, Bode A, Barthelmes F, Foerste C, Balmino G, Biancale R, Lemoine J-M, Loyer S, Perosanz F (2001) Earth Gravity Field Solutions from several months of CHAMP Satellite Data. EOS Trans AGU 82(47) (Fall Meet. Suppl): G4IC–02

Reigber C, Lühr H, Schwintzer P (eds) (2003) First CHAMP mission results for gravity, magnetic and atmospheric studies. Springer, Berlin Heidelberg New York

Schuh W (2002) Improved modelling of SGG-data sets by advanced filter strategies. In: Sünkel H (ed) From Eötvös to mGal+. Final report. ESA/ESTEC contract no. 14287/00/NL/DC, European Space Agency, Noordwijk

SID (2000). GOCE end to end performance analysis. Final report ESTEC contract no 12735/98/NL/GD, SID, Utrecht

Tapley B, Reigber C (1999) GRACE: a satellite-to-satellite tracking geopotential mapping mission. In: Marson I, Sünkel H (eds) Proceedings 2nd Joint Meeting of the International Gravity and the International Geoid Commission, Trieste, 7–12 September 1998. Boll Geofis Teor Appl 40: 291

Tapley B, Watkins M, Ries J, Davis G, Eanes R, Poole S, Rim H, Schutz B, Shum C, Nerem R, Lerch F, Marshall J, Klosko S, Pavlis N, Williamson R (1996) The joint gravity model 3. J Geophys Res, 101 (B12): 28029–28049

Tscherning C (1976) Covariance expressions for second and lower order derivatives of the anomalous potential. Rep 225, Department of Geodetic Science and Surveying, The Ohio State University, Columbus

Tscherning C (1993) Computation of covariances of derivatives of the anomalous gravity potential in a rotated reference frame. Manuscr Geod 8(3): 115–123

Visser P, van den IJssel J (2000) GPS-based precise orbit determination of the very low Earth orbiting gravity mission GOCE. J Geod 74(7/8): 590–602

Willemenot E (1999) Capacitive gradiometer: calibration and verification approach. Concluding tech rep RTS 19/3825 DMPH/Y, Onera, Châtillon